J. Membrane Biol. 46, 91–124 (1979)

Water Permeability of Yeast Cells at Sub-Zero Temperatures

Ronald L. Levin

Sibley School of Mechanical and Aerospace Engineering, Cornell University, Ithaca, New York 14853

Appendix I: Volumetric Changes in Yeast Cells during Freezing at Constant Cooling Rates

M. Ushiyama* and E.G. Cravalho**

Received 4 May 1978; revised 15 September 1978

Summary. A combined cryomicroscopic-multiple nonlinear regression analysis technique has been used to determine the water permeability of the yeast cell *Saccharomyces cerevisiae* during freezing. The time rate of change in volume of "supercooled" yeast cells was photographically monitored using a "cryomicroscope" which is capable of controlling in a programmable manner both the temperature and the time rate of change in temperature of the cell suspension being studied. Multiple nonlinear regression analysis together with a thermodynamic model of cell water transport during freezing was then used to statistically deduce the subzero temperature dependence of the cell water permeability. The water permeability process for *S. cerevisiae* being cooled at subzero temperatures was found to be rate-limited by the passage of water through either the plasmalemma, the cell wall, or a combination of these two permeability barriers. The hydraulic water permeability coefficient for yeast at 20 °C is approximately $1\text{–}2 \times 10^{-13}$ cm^3/dyne sec, if extrapolation from subzero temperatures to room temperature is permissible, while the apparent activation energy governing the permeability process at subzero temperatures is approximately 45–68 kJ/mol (11–16 kcal/mol).

In recent years, several models have been proposed to describe the physio-chemical events occurring during the freezing and thawing of biological cells and tissues as they relate to the redistribution of water with respect to both its physical state and location (Mazur 1963*b*, 1977; Mansoori, 1975; Silvares *et al.*, 1975; Levin, Cravalho & Huggins, 1976*a–b*,

* *Present address:* Cryogenic Engineering Laboratory, Department of Mechanical Engineering, MIT, Cambridge, MA 02139.

** *Present address:* MIT Health Sciences and Technology Program, MIT, Cambridge, MA 02139.

0022-2631/79/0046-0091 $06.80

1977*a–d*; Pushkar *et al.*, 1976). At the present time, however, only a qualitative comparison can be made between these theoretical analyses and the available experimental measurements of the intracellular water content of cells during freezing (Ushiyama *et al.*, 1973; Watson *et al.*, 1974; Leibo, Rall & Mazur, 1977; Knox and Diller, 1977; Leibo, McGrath & Cavalho, 1978), the transition cooling rate, e.g., the cooling rate above which the probability of intracellular ice nucleation for a given cell type is virtually 100% (Mazur, Leibo & Chu, 1972; Bank & Mazur, 1973; Bank, 1974; Diller, 1975; McGrath, Cravalho & Huggins., 1975; Leibo *et al.*, 1978), and the percent lysis of cells in strongly hypertonic solutions (Farrant & Woolgar, 1972*a–b*; Meryman, Williams & Douglas, 1977). This disparity is due to the fact that the theoretical analyses are only predictions, based on a number of simplifying assumptions (Mazur, 1977), of the events occurring during the freezing and thawing process. Moreover, they are predictions based upon experimental values for the water permeability of cell membranes, diffusivities of intracellular solutes, and other biophysical parameters obtained at or near room temperature (4 to 37 °C) and extrapolated to subzero temperatures (*see* Levin *et al.*, 1976*a*; Leibo *et al.*, 1977).

Mazur (1977) has considered the validity of the assumptions made in his original model (Mazur, 1963*b*) and acknowledges that a major source of error can be introduced by an incorrect estimation of hydraulic water permeability (L_p) and its temperature coefficient (b) at subzero temperatures. Unfortunately, even though the hydraulic water permeability of the cell membrane is the major parameter governing the behavior of cells and tissues during freezing and thawing, none of the above workers (Ushiyama *et al.*, 1973 – yeast; Watson *et al.*, 1974 – human RBC; Leibo *et al.*, 1977 – mouse ova; Knox & Diller, 1977 – HeLa cells) have utilized their cell dehydration and rehydration data to determine the cell water permeability during the actual freezing and thawing process. Recently, however, multiple nonlinear regression analysis (MNLRA) techniques for the determination of both water and nonelectrolyte permeability parameters by statistically fitting theoretical models for solvent and solute transport to sets of experimental data of cell volume as a function of time have been developed (Stusnick & Hurst, 1972; Levin & Solomon, 1978; Papanek, 1978). Consequently, using multiple nonlinear regression analysis and a thermodynamic model of the kinetics of cell water loss during freezing, we have statistically deduced from Ushiyama and Cravalho's cryomicroscopic measurements of the variation in cell volume of the yeast cell *Saccharomyces cerevisiae* during freezing (*see Appendix I*) the subzero temperature dependence of the water permeability of *S. cerevisiae*.

Description of Problem

When a cell suspension is cooled below its freezing point, the cells and their surrounding medium initially remain unfrozen due to "supercooling". Since more effective ice nucleators are present extracellularly, ice initially forms in the extracellular solution between -2 and $-15\,°C$, while the intracellular solution remains unfrozen and supercooled presumably because the cell membrane initially prevents the growth of ice into the cell (Mazur, 1960). The supercooled intracellular water therefore has a higher chemical potential than the water in the partially frozen extracellular solution which is in equilibrium with the ice phase. Chemical equilibrium can be achieved either by efflux of water out of the cell or by intracellular ice formation[1]. The manner in which equilibrium is achieved is a function of the rate at which the cell is cooled in relation to the capacity for water flux out of the cell. The amount of water that must be removed to re-establish chemical equilibrium will depend on the initial osmolality of the intracellular solution and the final temperature of the cell suspension. Whether this amount of water will be removed depends primarily on the permeability of the plasma membrane, the surface area available for efflux, and the cooling rate. If the flux is not adequate, which is usually the case for the faster cooling rates, then heat transfer will dominate over mass transfer and little, if any, cellular dehydration will occur. The intracellular solution will therefore become excessively supercooled and intracellular ice will form at the lower temperatures. If the flux is adequate, which is usually the case for the slower cooling rates, then mass transfer will dominate over heat transfer and the cell will dehydrate. Initially, intracellular freezing will be avoided as both the intracellular and extracellular solutions become more concentrated and equilibrate. However, eventually at the lower temperatures the intracellular and extracellular solutions will completely solidify due to the formation of eutectic mixtures rather than ice.

Mathematically, this cellular dehydration process during freezing can be modelled in the following manner.

Cell Volume Regulation

Although most solutions of biological interest are complex salt-protein-water solutions, let us consider the case of an intracellular solution

1 Chemical equilibrium can also be achieved by an influx of solute into the cell. Under normal circumstances, however, the permeability ω of most solutes is much less than the water permeability Lp. Hence, the net solute flux J_s is usually much less than the water flux J_w.

consisting of a single un-ionized solvent, w (water), and a single solute, s[2]. For this case, the volume of the cell V_c is related to the volume occupied by the cellular structural components (wall and membranes) and the intracellular components w and s such that:

$$V_c = V_{\text{solids}} + N_w \bar{v}_w + N_s \bar{v}_s \tag{1}$$

where N_w and $\bar{v}_w$, and N_s and $\bar{v}_s$, are, respectively, the number of moles and apparent molar volume of the water, and solute, inside the cell. For constant apparent molar volumes and a cell permeable to the solvent w but impermeable to the intracellular solute s and all extracellular solutes

$$dV_c/dt = \bar{v}_w(dN_w/dt) = -(\bar{v}_w \cdot J_w) A_c \tag{2}$$

where A_c is the surface area of the cell and J_w is the net flow of water *out of* the cell per unit surface area per sec. The cellular volume therefore varies with time such that

$$V_c(t) = V_{c)0} - \int_o^t (\bar{v}_w \cdot J_w) A_c \, dt \tag{3}$$

where $V_{c)0}$ is the initial cell volume and $(\bar{v}_w J_w)_{t=0} = 0$ because the intracellular and extracellular solutions are assumed to be in chemical equilibrium at $t=0$, that is, before extracellular nucleation occurs.

Water Flux

The water flux J_w is given by an expression of the form

$$J_w = \frac{L_p}{\bar{v}_w^2}(\mu_w^I - \mu_w^0) \tag{4}$$

where μ_w^I and μ_w^0 are, respectively, the chemical potentials of the water within the intracellular and extracellular solutions[3] and L_p is the hydraulic water permeability of the cell. The chemical potential for the water can be

2 Since the diffusion of ions of an electrolyte is restricted by the condition of electric neutrality, it is permissible to treat the partial volumes, concentrations, etc., as those of the electrolyte as a whole without considering the ν_s moles of ions per molecule as separate ionic quantities (*see* Robinson & Stokes, 1959, Chapter 2).

3 Actually, the driving force for the water flux is the chemical potential of the water at the solution-membrane interfaces. However, if we neglect the effects that compartmentali-

written as

$$\mu_w = \mu_w^*(T) + \bar{v}_w p + RT \ln a_w \tag{6}$$

where p is the hydrostatic pressure and a_w is the activity of the water in the solution. Since it is certainly reasonable to assume that there are no significant temperature gradients within the small cell suspension under consideration (Mansoori, 1975), we can let $\mu_w^*(T)|^I = \mu_w(T)|^0$. Hence,

$$\bar{v}_w J_w = -L_p \left[\Delta p - \frac{RT}{\bar{v}_w} (\ln a_w^I - \ln a_w^0) \right] \tag{7}$$

where

$$\Delta p = p^0 - p^I \tag{8}$$

represents the hydrostatic pressure difference across the cell membrane. For animal cells and isolated plant protoplasts, $\Delta p \simeq 0$ (House, 1974). However, for plant cells with intact cell walls, Δp represents the cell "turgor" pressure which is nonzero for unplasmolyzed cells. Now because of the elastic nature of plant cell walls, the intracellular hydrostatic pressure is usually dependent upon cell volume. In fact, changes in $p^I (dp^I)$ are usually related to the corresponding fractional changes in cell volume (dV_c/V_c) through an experimentally determinable cell wall parameter, the so-called "volumetric elastic modulus", ε (Philip, 1958; Dainty, 1976; Steudle, Zimmerman & Luttge, 1977):

$$\varepsilon = V_c \frac{dp^I}{dV_c}. \tag{9}$$

If ε is not a function of the cell volume, then the above equation can be integrated to yield the following expression for the cell turgor pressure:

$$\Delta p = -\varepsilon \ln \left(\frac{V_c}{V_{c)0}} \right) + \frac{RT}{\bar{v}_w} (\ln a_w^I - \ln a_w^0)|_0 \tag{10}$$

---

zation and the concentration polarization of solutes have on the water transport process, then we can assume that μ_w will be spatially uniform

$$\mu_w(\underline{r}, t) = \mu_w(t). \tag{5}$$

The water permeability L_p will therefore represent the overall water permeability of the cell and not of just the cell wall or membrane(s). For a detailed discussion of the effects of intracellular solute polarization upon the amount of water retained by cells during freezing, refer to Levin *et al.*, (1977*a*, *b*).

where $\Delta p \leqq 0$ and $V_{c)0}$ is the initial cell volume. Since for most plant cells, $|\varepsilon| \gg |\Delta p|$, the above equation can be approximated by the simplified relationship:

$$\Delta p = -\varepsilon \left(\frac{V_c}{V_{c)0}} - 1 \right) + \frac{RT}{\bar{v}_w} (\ln a_w^I - \ln a_w^0)|_0. \tag{11}$$

For the case of intracellular and extracellular solutions which can be considered to be dilute on both a mole and volume basis, Eqs. (7) and (11) reduce to the more common expressions

$$\bar{v}_w J_w = -L_p(\Delta p - \Delta \Pi) \tag{12}$$

and

$$\Delta p = -\varepsilon \left(\frac{V_c}{V_{c)0}} - 1 \right) + \Delta \Pi_0 \tag{13}$$

where $\Delta \Pi$ is the difference between the extracellular and intracellular solution osmotic pressures. The osmotic pressure Π is related to the water activity a_w and the number of moles of solutes within the solution such that

$$\Pi = \Phi RT \frac{N_s}{V_w} = -\frac{RT}{\bar{v}_w} \ln a_w \tag{14}$$

where Φ is the molal osmotic coefficient (Robinson & Stokes, 1959) and

$$V_w = V_c - V_b \tag{15}$$

where V_b is the apparent "non-osmotic" cell volume. In this instance, V_b is defined to consist of the volume of cell solids, including the volumes occupied by the intracellular solutes and the cellular structural material (wall and membranes), plus the volume of any water of hydration of the intracellular solutes and structural material which is "bound" too tightly to participate in osmotic phenomena and/or freeze (Levin *et al.*, 1976*b*). Consequently, V_w should be thought of as representing the volume of "free" cell water, i.e., the amount of water within the cell which is free to diffuse and/or leave the cell under a hydrostatic or osmotic pressure gradient and not the "total" cell water volume.

In order to evaluate Eqs. (12) and (14), values are also needed for a_w^0, the activity of the water in the extracellular solution. If the extracellular solution contains solutes, as would be true even for the case of deionized water, then some liquid solution will be present at temperatures above the

eutectic point. Therefore, by assuming that during the freezing process (i) once pure ice forms extracellularly, chemical equilibrium prevails between the solid and liquid phases in the extracellular medium so the latent heat of fusion of the solution can be approximated by the latent heat of fusion of pure water; and (ii) the composition of the liquid phase of the extracellular medium remains uniform, with no polarization of solutes taking place at either the external surface of the cell membrane or at the liquid-solid interfaces, a_w^0 can be shown to vary with temperature so that

$$\ln a_w^0 = 3.736 \times 10^3 [(1/T) - (1/T_o)] + 36.20 \cdot \ln(T/T_o) + 0.1025 (T_o - T) + 5.44 \times 10^{-5} (T^2 - T_o^2), \quad (16)$$

where $T_o = 273.15$ K (0 °C) (Dorsey, 1940; Levin *et al.*, 1976*b*). It should be noted that this expression for the water activity is independent of solution composition provided that the above mentioned conditions are satisfied. What will vary from one solution to another at any given temperature is the "composition" of that solution which will be determined by its phase diagram.

Water Permeability

If we consider the simplest case of the cell water permeability being rate-limited by the passage of water through the cell membrane, then the temperature dependence of L_p is given by

$$L_p = L_{p)T_g} \exp\left[-\frac{E_{L_p}}{R} \left(\frac{1}{T} - \frac{1}{T_g} \right) \right] \quad (17)$$

where $L_{p)T_g}$ corresponds to the water permeability at $T_g = 293.15$ K (20 °C) and E_{L_p} is the apparent activation energy for the permeation process. Typical values of L_p and E_{L_p} can be found in Table 1.

However, only for the simplest types of membrane systems can one expect an L_p temperature dependence such as that outlined above. For more complicated membrane systems, there may be any number of parallel and/or series resistances to the flow of water resulting in a complicated temperature and/or solute concentration dependence for the overall cell water permeability. Furthermore, any abrupt cell membrane lesion including phase changes of the lipoprotein portions of the cell membrane could manifest themselves as abrupt changes in the cell water permeability or solute permeability.[4]

4 For a discussion of possible cell membrane lytic events, *see* Wiest and Steponkus (1978). For a discussion of thermal events in biomembranes, *see* Melchior and Steim (1978).

Table 1. Typical cell water permeabilities

	$\frac{RT_g L_p}{\bar{v}_w}$ (10^{-3} cm/sec)	E_{L_p} (kcal/mol)	
Sea urchin eggs	0.32	13–17	McCutchen & Lucké (1932)
Erlich ascites tumor cells	3.7	9.6	Hempling (1960)
Nitella translucens	14.0	8.5	Dainty & Ginzburg (1964)
Human RBCs	24.6	3.3	Rich et al. (1968); Levin, Levin & Solomon (1978)
Ice	–	13–16	Dengel & Riehl (1963); Itagaki (1964)

Tg = 20 °C

Equation Nondimensionality

The above equations governing the movement of water into or out of cells can be handled more efficiently if they are rewritten as follows:

$$\frac{d\hat{V}_c}{dt} = \hat{L}_p \hat{A}_c \left(\frac{RT}{RT_g}\right)\left[\frac{\Delta p}{RT} - \Delta C\right] \tag{18}$$

where $\hat{V}_c$ and $\hat{A}_c$ are the cell volume and surface area relative to their initial values

$$\hat{V}_c = \frac{V_c}{V_{c)0}}; \qquad \hat{A}_c = \frac{A_c}{A_{c)0}} \tag{19}$$

$$\hat{L}_p = \frac{RT_g L_p A_{c)0}}{V_{c)0}}. \tag{20}$$

Hence, only relative cell volumes and surface areas as a function of time (temperature) are needed since uncertainties in values for $V_{c)0}$ and $A_{c)0}$ do not manifest themselves in the determination of $\hat{L}_p$, but only in the commonly reported value L_p. The osmotic pressure difference $\Delta\Pi$ is of the form

$$\Delta C = C^0 - C^I = \frac{\Delta\Pi}{RT} \tag{21}$$

where C^0 is the osmolality of the extracellular solution

$$C^0 = -\frac{1}{\bar{v}_w} \ln a_w^0 \tag{22}$$

and C^I is the osmolality of the intracellular solution

$$C^I = C_0^I \left(\frac{1 - \hat{V}_b}{\hat{V}_c - \hat{V}_b} \right) \tag{23}$$

C_0^I and C_0^0 are the initial osmolalities of the intracellular and extracellular solutions, respectively, and $\hat{V}_b$ is the relative nonosmotic cell volume:

$$\hat{V}_b = \frac{V_b}{V_{c)0}}. \tag{24}$$

The turgor pressure is of the form

$$\frac{\Delta p}{RT} = -\hat{\varepsilon} \left(\frac{RT_g}{RT} \right) \ln \hat{V}_c + \Delta C_0 \tag{25}$$

where

$$\hat{\varepsilon} = \frac{\varepsilon}{RT_g}. \tag{26}$$

Equilibrium Conditions

Finally, equilibrium is achieved when $d\hat{V}_c/dt = 0$ or $\Delta p/RT = \Delta C$. This results in the following transcendental equation for the equilibrium cell volume

$$-\hat{\varepsilon} \left(\frac{RT_g}{RT} \right) \ln \hat{V}_c + \Delta C_0 = C^0 - C_0^I \left(\frac{1 - \hat{V}_b}{\hat{V}_c - \hat{V}_b} \right) \tag{27}$$

which can be solved by an iterative procedure provided that C_0^I, C_0^0, $\hat{V}_b$, $\hat{\varepsilon}$ and T are known. For $\hat{\varepsilon}/C^0 \ll 1$ and $\Delta C_0/C^0 \ll 1$, the above equation reduces to the familiar Boyle-Van't Hoff relationship

$$\hat{V}_c = \frac{C_0^I}{C^0}(1 - \hat{V}_b) + \hat{V}_b. \tag{28}$$

MNLRA Technique

Although this set of equations (16–26) has been solved exactly for the special case of cells placed in a hypertonic or hypotonic solution at a constant temperature (Sidel & Solomon, 1957), there is no general

analytical solution for the case of cell cooling or warming at subzero temperatures. We have therefore followed the lead of Stusnick and Hurst (1972), Levin and Solomon (1978) and Papanek (1978) in applying the numerical nonlinear fitting technique of Marquardt (1963) and Bevington (1969) to obtain "best-fit" values for the permeability parameters, as well as estimates of their accuracy by statistically fitting the cell membrane transport equations to sets of experimental data of cell volume as a function of time.

Briefly, the best-fit values of a set of m parameters, $a_j (j=1,m)$, in a function

$$V_c(t)=f(a_1,\ldots,a_m,t) \tag{29}$$

which describes a set of n data points, $[V_{ci},t_i]$ $(i=1,\ldots,n)$, are those for which the variance between the experimental V_{ci} and theoretical $V_c(t_i)$ values[5] of the cell volume

$$\mathrm{VAR}(a_1,\ldots,a_m)=\frac{\sum_i \frac{1}{\sigma_i^2}(V_{ci}-V_c(t_i))^2}{\sum_i 1/\sigma_i^2} \tag{30}$$

is a *minimum*. The σ_i's are the estimates of the error in the data point V_{ci} resulting from the inherent uncertainty in determining cell volume as a function of time and from any averaging techniques that may be employed. The variance will be an extremum if

$$\frac{\partial \mathrm{VAR}}{\partial \mathrm{a}_j}=0 \qquad j=1,\ldots,m. \tag{31}$$

However, since the function $f(a_1,\ldots,a_m,t)$ is nonlinear in the parameters a_j, an iteration procedure, which repeatedly improves by an amount δa_j on some initial estimation of the parameters, a_j^o, must be used to estimate the values of the parameters which minimize the variance (Bevington, 1969, Chapter 11). One such method is that outlined by Marquardt (1963) in which the parameter increments δa_j are defined by the matrix equation

$$\underline{A'}\,\underline{\delta a}=\underline{B} \tag{32}$$

5 The theoretical values of cell volume as a function of time are found by numerically integrating Eq. (3), using either a second- or fourth-order Runge-Kutta routine with a small enough step size to produce suitable accuracy for the calculation of the membrane parameters.

with the resulting solution

$$\underline{\delta a} = (\underline{A}')^{-1}\underline{B}\,. \tag{33}$$

Here the elements of the $m \times m$ symmetric $\underline{A}'$ matrix and $m \times 1$ column matrix $\underline{B}$ are given by

$$\begin{aligned} A'_{jk} &= A_{jk}(1+\lambda) \qquad j=k \\ A'_{jk} &= A_{jk} \qquad\qquad\quad j \neq k \end{aligned} \tag{34}$$

where

$$A_{jk} = \sum \frac{1}{\sigma_i^2}\left\{\frac{\partial f}{\partial a_j}(a_1^o, \ldots, a_m^o, t_i)\cdot\frac{\partial f}{\partial a_k}(a_1^o, \ldots, a_m^o, t_i)\right\} \tag{35}$$

$$B_j = \sum \frac{1}{\sigma_i^2}\{V_{c_i} - f(a_1^o, \ldots, a_m^o, t_i)\}\frac{\partial f}{\partial a_j}(a_1^o, \ldots, a_m^o, t_i) \tag{36}$$

The constant λ controls the relative weighting that the search procedure gives to the so-called "gradient" ($\lambda \gg 1$) and "linearization" ($\lambda \ll 1$) methods (Bevington, 1969).

One starts with an initial set of estimates for the permeability parameters, a_j^o, and using a relatively large value of $\lambda(10^{-3})$, computes a set of parameter increments, δa_j, which define a second set of parameters, $a_j^o + \delta a_j$. This iteration process is continued until the minimum variance is reached. At each iteration the corresponding value of the variance is computed and λ is reduced only if its reduction produces a smaller value of the variance than in the previous set. The iterative procedure is terminated when the percent change in the variance is less than some specified level (usually 0.05 %). The uncertainties in the final values of the parameters are then computed (Bevington, 1969):

$$\sigma_{a_j}^2 = [A'_{jj}]^{-1} \tag{37}$$

and the experimental and theoretical values of the cell volume as a function of time and temperature are plotted to visually confirm the "goodness of fit".

Application of Model and MLNRA Technique

The model and method of analysis presented above is applicable to a wide variety of physical situations. However, since we are interested in determining the water permeability of yeast at subzero temperatures, some

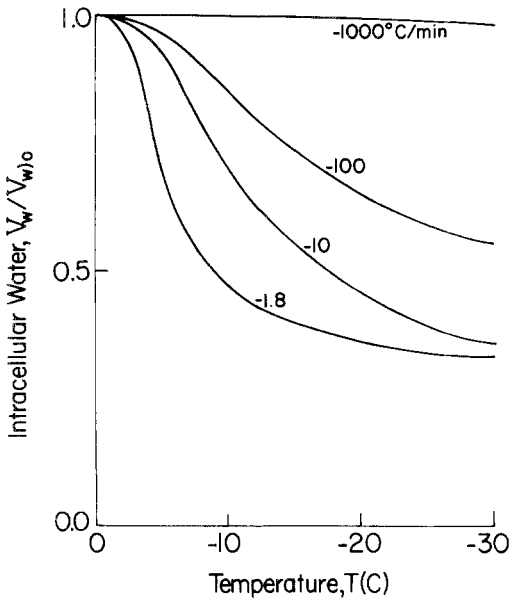

Fig. 1. Percent intracellular water content of yeast cells *(S. cerevisiae)* cooled at constant rates, as experimentally determined by Ushiyama (1973)

remarks concerning the experimental data of Ushiyama and Cravalho (Ushiyama, 1973; Ushiyama *et al.*, 1973) and the biophysical parameters used in our analysis are in order before presenting our results.

Briefly, Ushiyama and Cravalho photographically measured the changes in volume of cells of the diploid yeast *Saccharomyces cerevisiae* suspended in distilled water and cooled at rates of 1.8, 10, 100, and 1000 °C/min between 0 and −30 °C using a cryomicroscope system equipped with a "convective" cooling stage (Diller & Cravalho, 1970). Details of their experimental procedure and a brief discussion of their results can be found in *Appendix I.* Their measurements of the percent intracellular water retained by the yeast are presented in Fig. 1. A comparison of these experimental results can be made with the theoretical predictions of Mazur (1963*b*) which are presented in Fig. 2. Qualitatively, the agreement between Ushiyama and Cravalho's experimental data and Mazur's theoretical predictions are good; quantitatively, they are not. This quantitative disparity is due to our findings that the apparent water permeability activation energy for yeast is larger than the value of 20 kJ/mol (4.9 kcal/mol) assumed by Mazur (1963*b*) and that Mazur's predictions (1963*b*, 1965) are valid only for animal cells or isolated plant protoplasts and not for cells with intact cell walls like yeast and therefore possessing a nonzero turgor pressure.

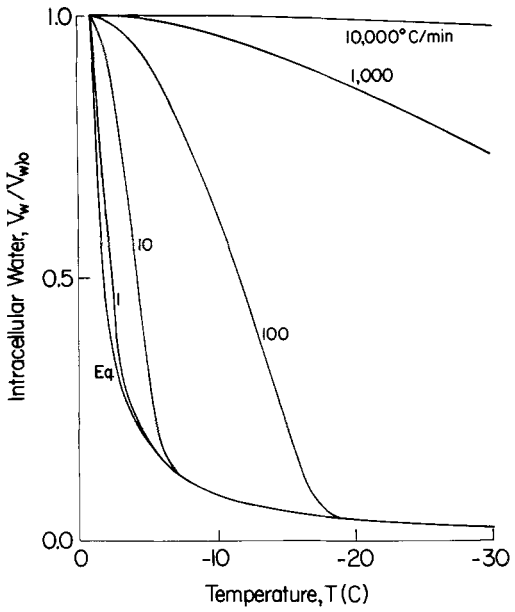

Fig. 2. Percent intracellular water content of yeast cells as theoretically determined by Mazur (1963*b*)

Since relative cell volume ($\hat{V}_c$) as a function of time (temperature) is required for the application of the regression analysis technique outlined above, Eq. (A2) was used to convert the " % intracellular water content" data as presented by Ushiyama and Cravalho (*see* Fig. 1) into relative cell volume data (*see* Fig. 3). The variation of relative cell volume with subzero temperature for the cooling rates[6] of 1.8, 10, and 100 °C/min as depicted in Fig. 3 should therefore represent the actual volumetric data originally deduced by Ushiyama and Cravalho from their measurements of the major and minor axes of the ellipsoidal yeast cells. These three curves will form the basis of the following discussion.

As can be seen in Fig. 3, the largest change in yeast cell volume occurs for the lowest cooling rate while the smallest change in volume occurs for the highest cooling rate. The qualitative behavior is to be expected and has been observed for a large number of different cell types (RBC—Watson, 1974; Mouse ova—Leibo *et al.*, 1977). For the yeast cells we are considering it took 1,000 sec to reduce the temperature from 0 to −30 °C at the 18 °C/min cooling rate but only 18 sec at the 100 °C/min cooling rate. This 50-fold difference in cooling rate therefore manifests itself directly as a 50-fold difference in the time allowed for water to leave the cells.

6 The volumetric data obtained for $B = -1{,}000$ °C/min will not be analyzed since little, if any, change in volume occurred in the temperature range studied.

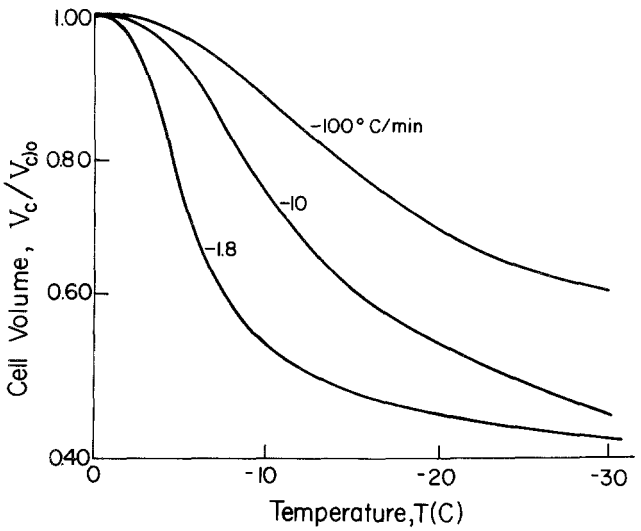

Fig. 3. Relative cell volumes of yeast cells *(S. cerevisiae)* cooled at constant rates. Recomputed from the experimental data of Ushiyama (1973)

Quantitatively, the data of Ushiyama and Cravalho at the cooling rates of 10 and 100 °C/min seem also to be acceptable. For the case of *S. cerevisiae* cooled at about 50 °C/min (between −5 and −25 °C) and freeze substituted at −32 °C or cooled at about 280 °C/min (between −5 and −65 °C) and freeze substituted at −65 °C, Mazur (1961*b*) found cells having relative volumes of 0.44 and 0.49, respectively. This is in very good agreement with the relative volumes at −30 °C of 0.45 and 0.61 measured by Ushiyama and Cravalho for the respective cooling rates of 10 and 100 °C/min. At the slower cooling rates, however, there is a quantitative discrepancy between the experimental findings of Ushiyama and Cravalho and Mazur. For yeast cooled at about 1 °C/min and freeze substituted at −32 °C, Mazur (1961*b*) measured a relative cell volume of 0.31. This is to be contrasted with Ushiyama and Cravalho's measurement of 0.43 at −30 °C for a 1.8 °C/min cooling rate. Possible reasons for this discrepancy will be discussed later.

Unfortunately, none of the biophysical parameters necessary for the application of the model were measured by Ushiyama and Cravalho at the time they performed their experiments. However, since their strain of *S. cerevisiae* were obtained from Mazur and were cultured and prepared for the experiments according to the method developed by Mazur (1961*a*), we have relied, where possible, upon the biophysical parameters determined by Mazur and his colleagues. The biophysical parameters used in the analysis of Ushiyama and Cravalho's data are summarized in Table 2. For the initial

yeast cell volume and surface area we have chosen the values of 96 μm^3 and 100 μm^2, respectively. These are the most recent mean values determined by Mazur (1963*a*). The value of $V_{c)o} = 96\,\mu m^3$ is also within the range of 50–130 μm^3 observed by Ushiyama and Cravalho for the initial cell volume of their yeast. Furthermore, as we have previously stated, these values affect only the value of $L_{p)T_g}$ which we shall report and not the nondimensional value $\hat{L}_p$ (*see* Eq. (20)) which is used in the regression analysis. Finally, since Ushiyama and Cravalho did not report their raw data (measurements of major and minor axes), we have assumed that the relative cell surface area varied as the 2/3rds power of the relative cell volume. Assumption of a constant cell surface area during cell shrinking, however, does not dramatically affect the results presented below.

In his studies of *S. cerevisiae* by differential thermal analysis and conductometry, Mazur (1963*a*) assumed a relative protoplast (vacuole plus cytoplasm) water volume of 0.76. This value for $\hat{V}_{w)o}$ corresponds to an osmotic inactive volume of $\hat{V}_b = 0.24$, which we have employed in our analysis. It should be noted that this assumed value for the osmotic inactive volume is also close to the values of 0.238, 0.24, and 0.30, which can be deduced respectively from the data of Ørskow (1945), Conway and Downey (1950), and Wood and Rosenberg (1957).

For the volumetric elastic modulus of the yeast cell wall, ε, we assumed a value of zero, even though a value of 4.7 MPa (680 psi) can be deduced from the data of Conway and Downey (1950) and Conway and Armstrong (1961) on the distensibility of the yeast cell wall[7]. Both Steudle *et al.* (1977) and

---

7 Using the data obtained by Conway and Downey (1950) for the variation of yeast cell volume in the presence of the nonpenetrating sugars D-galactose and L-arabinose in the osmolality range 38 to 695 mosmol/liter, Conway and Armstrong (1961) derived the following linear relationship between V_w and ΔC (in mosmol/liter):

$$\frac{V_w^I}{M} = -340 \times 10^{-6}\,\Delta C + 0.295 \tag{38}$$

where M was the mass of yeast in the cell suspension being studied. Now $M = dV$ where d is the density of the yeast cell suspensions ($d = 1.06$ kg/liter solution) and V is the total volume of their suspension. Since Conway and Downey (1950) determined that $V_w/M = 0.79$ liter/kg (total water in cell suspension) and $V_w^0/M = 0.30$ liter/kg (extracellular plus cell wall water), the above equation can be placed in the form:

$$\hat{V}_c = -528 \times 10^{-6}\,\Delta C + 0.698. \tag{39}$$

Upon comparison with Eq. (27), this equation not only yields a value of 572 mosmol/liter for the intracellular yeast osmolality under full turgor conditions ($C^0 = 0$ and $\hat{V}_c = 1.0$) and a value of $\hat{V}_c^p = 0.698$ for the relative yeast cell volume at incipient plasmolysis ($\Delta C = \Delta p = 0$), but also a value for the reduced volumetric elastic modulus, $\hat{\varepsilon} = (1920 \pm 20)$ mosmol/liter which corresponds to a value of 4.7 MPa (680 psi) for ε.

Table 2. *S. cerevisiae* biophysical parameters

Initial cell volume	$V_{c)o}$	96 μm³
Initial cell surface area	$A_{c)o}$	100 μm²
Osmotically inactive volume	$\hat{V}_b$	0.240
Volumetric elastic modulus	ε	0
Room temperature	T_g	293.15 K (20 C)
Extracellular solution nucleation temperature	T_o	273.15 K (20 C)
Relative cell volume at T_o	$\hat{V}_{c)o}$	1.00
Relative cell surface area at T_o	$\hat{A}_{c)o}$	1.00
Osmolalities at T_o		
Intracellular	C_o^I	540 mosmol/liter
Extracellular	C_o^0	0.00
Cell turgor pressure at T_o	Δp_o	1.33 MPa (13.10 atm)

Kelly, Kohn and Dainty (1963) have found that for a number of different types of cells ε depends strongly on both turgor pressure and cell volume. The conclusion reached by Steudle and colleagues is that the $\varepsilon(p)$ characteristics (rapidly decreasing ε as $\Delta p \to 0$) and the $\varepsilon(V)$ characteristics (increasing ε with increasing cell size at a given turgor pressure) of all plant cells are similar. Evidence of a complicated cell volume and/or turgor pressure dependence of the cell wall elastic modulus for yeast can be deduced from the data of Mazur (1961*b*). First, nonviable frozen-thawed yeast (survival percentage $<0.1\,\%$) were found to have volumes of only approximately 55 % of normal. If we assume that the turgor pressure of these nonviable cells has been eliminated due to the destruction of the plasma membrane, then presumably the cell wall is no longer under elastic tension. This 55 % relative cell volume corresponds to a value for ε of 2.2 MPa (320 psi), slightly less than half of the value that can be deduced from the data of Conway and his colleagues. Secondly, freeze-substituted yeast originally cooled at various rates to temperatures below −30 °C were found to have volumes of less than 50 % of normal. For slowly cooled cells at low temperatures, the cell wall might therefore continue to shrink because of the adhesion between it and the plasma membrane. Consequently, because of the probably complicated turgor pressure, temperature, and cell-volume dependence during cell freezing of the volumetric elastic modulus, we assumed that $\varepsilon \equiv 0$ during the entire cooling process. It should be noted, however, that a value for ε of zero *does not* correspond to a value of zero for the cell turgor pressure [*see* Eq. (13)].

The intracellular solution osmolality of the yeast cells under full turgor, i.e., for cells suspended in distilled water, was assumed to be 540 mosmol/liter. This value was experimentally determined by Mazur (1963*a*) using

DTA and is supported by the work of other investigators. Eddy and Williamson (1957) found that the isosmotic suspending solution for yeast protoplasts was 500 mosmol/liter. Conway and Armstrong (1961) estimated the intracellular osmolality of yeast to be 590 mosmol/liter on the basis of cryoscopic measurements and the summation of the colligative osmotic contributions of the known constituents of yeast protoplasm. Furthermore, as stated above, a value of 572 mosmol/liter for the intracellular osmolality of yeast at full turgor pressure can be deduced from the data of Conway and Downey (1950) on the osmotic behavior of intact cells. This assumption of 540 mosmol/liter for the intracellular osmolality of the yeast cell *S. cerevisiae* under full turgor conditions results in an assumed value of 1.33 MPa (13.1 atm) for the cell turgor pressure at 0 °C.

Finally we have assumed, on the basis of Fig. 1, that the extracellular solution exhibited no supercooling and therefore that the "freezing" process began at 273.15 K (0 °C). We also assumed that, since the yeasts were suspended in distilled water, no eutectic mixture formed extracellularly within the temperature range of 0 to −30 °C.

Results and Discussion

Using the biophysical parameters summarized in Table 2 and the volumetric data of Ushiyama and Cravalho shown in Fig. 3, the thermodynamic model of cell volume regulation and the multiple nonlinear regression analysis technique outlined above were employed to determine the hydraulic water permeability of the yeast *S. cerevisiae* during cooling at subzero temperatures. For the case where the temperature dependence of L_p is assumed to be governed by the simple Arrhenius expression [Eq. (17)], the resulting values for $L_{p)T_g}$ ($T_g = 20$ °C) and the apparent permeability activation energy E_{L_p} are summarized in Table 3. A comparison of the theoretical and experimental variation of cell volume as a function of subzero temperature for each of the three cooling rates analyzed can be found in Fig. 4. Although the agreement between theoretical and experimental cell size is very good in all cases, the resulting values for L_p vary considerably (*see* Table 3). We believe, however, that these large variations, especially in the values for the apparent activation energy, probably reflect the inherent experimental uncertainties in the determination of cell diameter (volume) as a function of time by Ushiyama and Cravalho and their inability to observe whether or not plasmolysis occurred, rather than by inaccuracies in the thermodynamic model or biophysical parameters

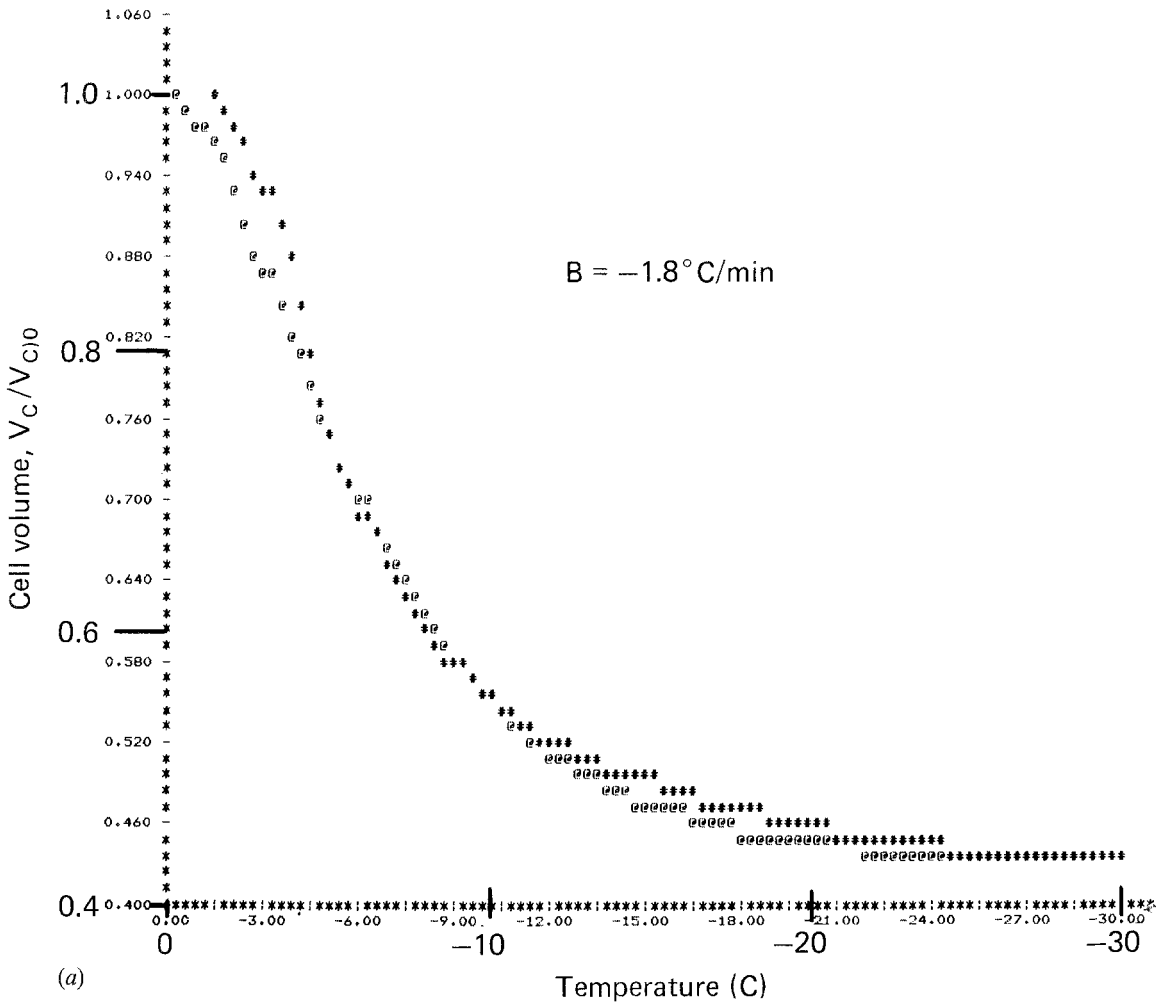

Fig. 4. (*a–c*): Theoretical (@) and experimental (# values for the volume of yeast cells (*S. cerevisiae*) cooled at constant rates. The experimental data corresponds to the data of Ushiyama (1973), while the theoretical data is computed on the basis of the "best fit" values for the permeability parameters listed in Table 3

used in the analysis or in the nonlinear regression analysis technique used to "fit" the experimental data. This opinion is based upon the following observations.

First, the purpose of Ushiyama and Cravalho's study was to demonstrate the "feasibility" of using a cryomicroscope to observe changes in cell size during freezing at known cooling rates. That is, data was collected on the volumetric changes in *S. cerevisiae* so that a qualitative, not quantitative, comparison could be made between their work and the earlier theoretical predictions of Mazur (1963*b*). Despite this, the volu-

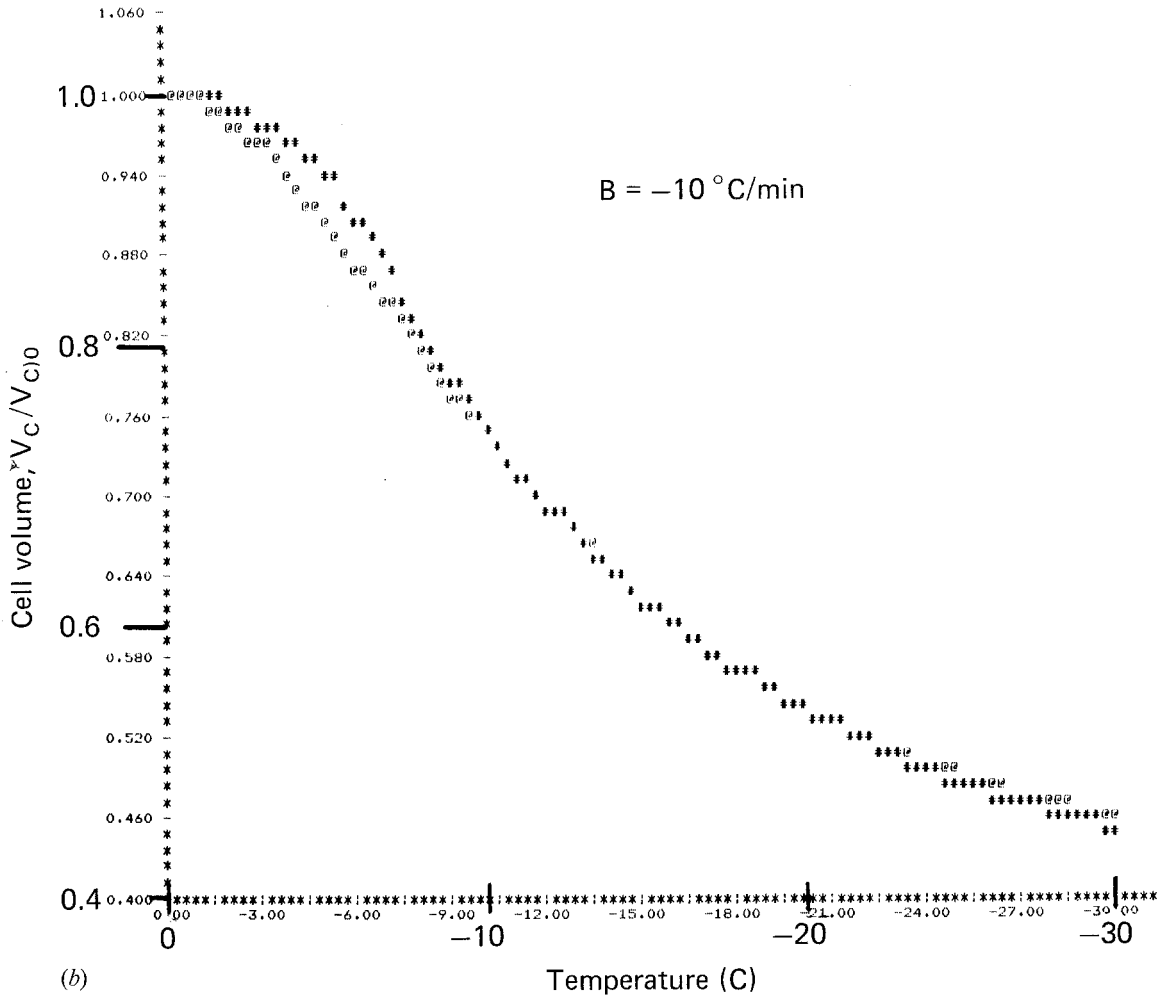

(*b*)

metric measurements of Ushiyama and Cravalho at the cooling rates of 10 and 100 °C/min do yield physically reasonable sets of permeability parameters. The $L_{p)T_g}$ values of 2.3×10^{-13} and 1.2×10^{-13} cm^3/dyne sec are very close to the value of 2.5×10^{-13} cm^3/dyne sec which Mazur (1963*b*) deduced from the yeast permeability studies of Ørskow (1945). Furthermore, the apparent activation energy values of 45.3 and 67.9 kJ/mol (10.8 and 16.2 kcal/mol) are within the typical range for biological membrane water permeability activation energies (*see* Table 1). In fact, the only physically unreasonable value obtained in the reduction of the yeast cell data is the value of 143 kJ/mol (34.1 kcal/mol) for the 1.8 °C/min cooling velocity case. We believe though that this unrealistically

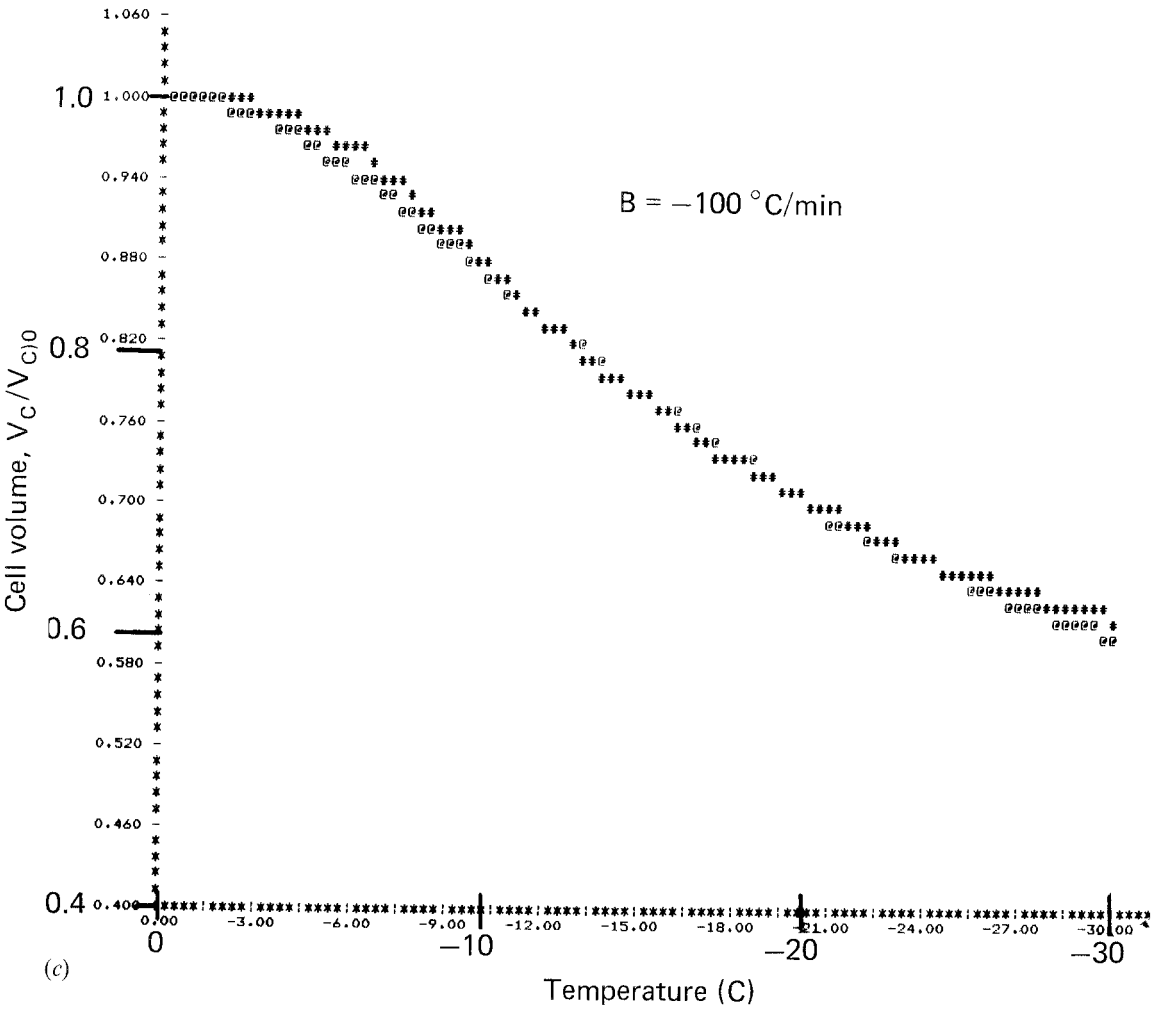

(*c*)

Table 3. Water Permeability

B °C/min	$L_{p)20c}$ 10^{-13} cm^3/dyne sec	E_{L_p} kJ/mol (kcal/mol)	Variance
−100	2.31 ±0.01	45.3 ±0.1 (10.83 ±0.03)	7×10^{-5}
−10	1.21 ±0.03	67.9 ±0.3 (16.22 ±0.08)	2×10^{-4}
−1.8	8.2 ±0.2	142.7 ±0.4 (34.1 ±0.1)	4×10^{-4}

Note: The probable errors quoted for the L_p's and E_{L_p}'s are computed on the basis of the variance between the experimental and theoretical values of cell volume as a function of time (*see* Bevington, 1969).

large value for E_{L_p} is a result of the seemingly large cell volume observed by Ushiyama and Cravalho at $-30\,°C$ (*cf.* Mazur, 1961*b*). Indeed, the initial slope of the shrinking curve for the $-1.8\,°C/min$ case can be adequately fitted by a $L_{p)T_g}$ value and E_{L_p} value within the ranges obtained for the other two cases. The tail of this theoretical cell volume *vs.* temperature curve at the low temperatures ($T \lesssim -10\,°C$), however, more closely corresponds to the relative cell volume measurements of 0.32 obtained by Mazur (1961*b*) at $-32\,°C$ for a cooling rate of $1\,°C/min$ rather than the 0.43 value observed by Ushiyama and Cravalho. This volume discrepancy could be due to the inability of Ushiyama and Cravalho to detect plasmolysis at cell volumes less than 50% of normal because of both the optical limitations of light microscopes and the obscuration of their field of view by extracellular ice. However, the electron micrographs of Bank and Mazur (1973) and Bank (1973) seem to indicate that yeast cells do not plasmolyze during either rapid or slow freezing even though their relative cell volumes at low temperatures for slow cooling rates are less than their supposedly plasmolytic volume of 50 to 70%. Furthermore, as we have already mentioned, Mazur (1961*b*), using a freeze-substitution technique, has measured yeast cell volumes of less than 50% at low temperatures. Although Mazur (1961*b*), like Ushiyama and Cravalho, was unable to visualize either the occurrence or nonoccurrence of plasmolysis, his volumes for yeast frozen at potentially viable rates are definitely less than his volumes for nonviable frozen-thawed yeast. Therefore, even though plasmolysis of highly shrunken yeast during freezing, resulting in the continuing osmotic shrinking of the protoplast while the volume enclosed by the cell wall remains relatively constant, cannot be ruled out, there is no direct experimental evidence to confirm that it does indeed occur. We are still faced with the fact that the cell volume of yeast cooled to approximately $-30\,°C$ at $1\,°C/min$ as measured by Ushiyama and Cravalho is still 35% larger than Mazur's seemingly more reasonable value.

Secondly, except for (i) a possible complicated dependence of L_p upon temperature *and* both intracellular and extracellular solution osmolalities, or (ii), a phase change[8] occurring within the yeast cell membrane(s) or wall at the lower cooling rates (and not at the higher cooling rates) because of the relatively longer exposure of the cells to subzero temperatures, an increase in the apparent water permeability activation energy

8 The phase change could be of the form of a membrane solidification phenomenon which results in an increase in the resistance to the passage of water out of the cell or in the ability of extracellular solutes to enter the cell.

with decreasing cooling rate cannot be explained in light of any other assumptions which we have made about the data of Ushiyama and Cravalho itself, the thermodynamic model used to reduce the data or the biophysical parameters used in the analysis (*see Appendix II*).

Conclusion

On the basis of these reasonable but scattered results, we believe that the water permeability process for the yeast cell *S. cerevisiae* being cooled at subzero temperatures is rate-limited by the passage of water through either the plasmalemma, the cell wall, or a combination of two permeability barriers. The hydraulic water permeability coefficient for yeast at 20 °C is approximately $1-2\times10^{-13}$ cm^3/dyne sec, if extrapolation from subzero temperatures to room temperature is permissible, while the apparent activation energy governing the permeability process at subzero temperatures is approximately 45–68 kJ/mol (11–16 kcal/mol). Further experiments on both intact yeast cells and yeast protoplasts should improve the accuracy of these observations and determine whether the yeast cell wall exerts a rate-limiting effect upon the overall permeation process.

Appendix I

Volumetric Changes in Yeast Cells during Freezing at Constant Cooling Rates

M. Ushiyama and E.G. Cravalho

Materials and Methods

Yeast cells of the strain *Saccharomyces cerevisiae* (NRRL Y-2235 Diploid) were obtained through the kindness of Dr. Peter Mazur of Oak Ridge National Laboratory (Oak Ridge, Tenn.). They were cultured and prepared for the experiments according to the method developed by him (Mazur, 1961*a*). Using the cryomicroscope system constructed by Diller *et al.* (1970, 1976) and Ushiyama (1973), approximately $1\sim2\,\mu$l of the cell suspension ($\sim2\times10^8$ cells/ml distilled water) were placed on the cryostage at room temperature and covered by a standard coverslip. Cooling rates were selected on the basis of the theoretical data available from Mazur's analytical model (*see* Fig. 2 and

Mazur, 1963*b*), namely, from -1 to $-1{,}000$ °C/min by increments of the factor of 10. Specifically, the selected cooling rates were 1, 10, 100, and 1,000 °C/min. However, due to electronic difficulties within the temperature control unit, the slowest rate attained was -1.8 °C/min.

Beginning at room temperature, the specimen was slowly cooled to just above 0 °C where it was held for 5 min to allow the cells to reach equilibrium with their environment prior to the freezing process. The cooling rate was selected and the final temperature of the cooling protocol was programmed to be -30 °C. The freezing protocol was then initiated.

Sequential photographs were taken starting at 0 °C to facilitate the correlation of the cell volume to its corresponding temperature with a Nikon F camera equipped with a Nikon F36 motor drive and intervalometer model NC-1 (Nikon, Inc., Garden City, N.Y.). The intervalometer was programmed to fire the shutter at the time interval corresponding to a temperature change of 1 °C except for the experiments where the cooling rate was 1,000 °C/min, for which the shutter was fired at the rate of three pictures per sec. For this last case, the temperature at which the photograph was taken was determined by dividing the temperature change for the entire sequence by the number of photographs taken except for the first one taken at 0 °C (considered to be the zeroth photograph) and by multiplying the sequence number of the photograph of interest.

Positive enlargements of the size 20.3×25.4 cm (8×10 in) were obtained at constant magnification from the negatives. Each enlargement was correlated to its corresponding temperature, and several cells, appearing consistently throughout the sequences, were measured along their major and minor axes. From these measurements, cell volumes were calculated by using a prolate spheroid model (or spherical model if major and minor axes were identical), and the following formula:

$$V_c(T) = \frac{\Pi}{6} x\, y^2 \tag{A1}$$

where $V_c(T)$ is the volume of a cell at temperature T, and x and y are, respectively, the lengths of its major and minor axes. These cell volumes were converted to percent intracellular water content by assuming that 84.6 % of the volume of the cell is occupied by water (Mazur, 1973*b*). Thus,

$$\frac{V_w(T)}{V_w(T_o)} = \frac{V_c(T) - 0.154\, V_c(T_o)}{0.846\, V_c(T_o)} \tag{A2}$$

where $T_o = 273.15$ K (0 °C). Points were plotted for the % intracellular water content *vs.* temperature for each cooling rate. A curve was fitted to each graph by sight and a composite graph was drawn (*see* Fig. 1) to compare the effect of the cooling rates with that of Mazur's analytical model (*see* Fig. 2).

There were four main difficulties encountered with the technique described above. First, when the camera was rigidly attached to the microscope, the vibrations created by the camera rendered the photomicrographs worthless because of blur. This difficulty was eliminated by mounting the camera on a separate, rigid stand so that the vibrations were totally damped.

Second, when the temperature of the specimen was altered, the focus of the microscope objective shifted. Consequently, the focus was maintained by finely and continuously adjusting the microscope focusing knob during the freezing protocol.

Third, the temperature difference across the stage was found to be of the order of 20 K due to its large dimensions ($d \sim 25$ mm). However, since the specimen was placed at the thermocouple junction and occupied a comparatively small area in relation to the freezing stage, it is assumed that the effects of the temperature gradients were negligible.

Finally, due to the temperature gradient across the freezing stage, cell movement was encountered. This movement was particularly pronounced at the higher cooling rates and numerous runs were needed until a successful sequence was obtained that showed cells appearing consistently in every photograph. Precaution was taken to wait until the movement had subsided, but this did not entirely eliminate the difficulty.

All of the photomicrographs were taken with a micrometer eyepiece in position, i.e., calibrated divisions appeared on all of the photographs. By knowing the correlation between a division and its corresponding actual scale, absolute cell volumes were calculated. The initial cell volumes ranged between 50 and 130 μm^3, which proved to be in the neighborhood of the initial cell volume of 88 μm^3 assumed by Mazur (1963*b*) in his analytical calculations.

Results

Figure 1 presents the results of the experiments where the percent intracellular water content is plotted against the temperature for each of the four cooling rates. It shows that the maximum water loss occurs at the slowest cooling rate, namely, at 1.8 °C/min. At that cooling rate, the temperature rate of cell water loss (i.e., the change in water content of the cell per unit change of temperature) is initially very high and begins to decrease by the time the cells reach −8 °C.

By the time −20 °C is reached, minimum water content has been attained at approximately 35% and the rate of cell water loss is essentially zero. As the cooling rate increases, this water loss is less rapid and the minimum water content is not attained by the time −30 °C is reached when the observation was terminated. At the cooling rate of 1,000 °C/min, the cells appear to retain most of their water. However, there were evidences of cell crenation from the photomicrographs taken at this cooling rate. Thus, it is evident that the slower the cooling rate, the greater the water loss per unit temperature change. In addition, for a given temperature, the slope of the curve (dV/dT) is more sensitive to the change in cooling rate at slow rates.

Supercooling of the extracellular medium was observed at cooling rates higher than 100 °C/min, at which time the phase change appeared to occur between −5 and −7 °C, depending on the individual run.

Intracellular ice formation was not observed between 0 and −30 °C for any of the cooling rates studied (1.8 to 1,000 °C/min). Viability (survival) assays were also not performed.

Appendix II

Evaluation of Assumptions Used in Data Reduction Procedure

1. Constant Cooling Rate and Temperature Uniformity within Cell Suspension

In the analysis presented above, it was assumed that the cooling rate of the cell suspension was constant and that the temperature of the cell suspension was uniform. Although one might think that such an assumption would be experimentally difficult to achieve, Cravalho and colleagues at MIT with the use of a "cryomicroscope" have been able to maintain specimen temperature and their time rate of change to within very close tolerances ($\pm 1\%$) of a preprogrammed value (Diller *et al.*, 1976). Although temperature gradients do exist on the various cold stages used with this type of microscope, care is usually taken to analyze only those cells immediately in the vicinity of the temperature measuring thermocouple which is placed directly in the cell suspension. Ushiyama and Cravalho followed "normal operating procedure" and measured the volumes of those cells only in the immediate vicinity of the thermocouple. Likewise, we feel that it is reasonable to assume that extracellular ice nucleation occurred within a few degrees of the normal freezing point of pure water (0 °C) and that sufficiently small samples of yeast cell suspensions were used so that the heat of fusion released upon extracellular freezing could be removed by the cold stage's refrigeration system.

Regarding our assumption of thermal equilibrium within the immediate vicinity of the cell, temperature uniformity both intracellularly and extracellularly, is readily achieved at the cooling rates used. The governing nondimensional parameter for heat transfer in a sphere having a diameter d, initial temperature T_o, thermal diffusivity $D^T(=k/\rho c_p)$ and with its surface being cooled (or warmed) at a constant rate B is the Predvoditelev number (Pd) (Luikov, 1968):

$$Pd_o = \frac{|B| d^2}{4 D^T T_o}. \tag{B1}$$

If $Pd \gg 1$, then the heat transfer process is limited by the thermal diffusion of heat within the system and we should expect a nonuniform temperature profile to exist within the sphere. On the other hand, if $Pd \ll 1$, then the heat transfer process is limited by the ability of the refrigeration network to remove heat from the system and we should

expect that a uniform temperature profile would exist within the sphere. For water at 0 °C and ice between 0 and −30 °C, D^T equals 1.36×10^{-3} and 1.1×10^{-1} cm^2/sec, respectively (Mazur, 1963*b*; Dorsey, 1940). Hence for a sphere with a 50 μm diameter, which is approximately ten times the diameter of an average yeast cell, the Predvoditelev number for water and ice are, respectively:

$$P d_o^w = \frac{|B|}{3.6 \times 10^6} \qquad P d_o^I = \frac{|B|}{2.9 \times 10^7}$$

where B is in °C/min. Consequently, even for cooling rates of the order of 10^4 °C/min, temperature uniformity should be maintained extracellularly. Intracellularly, Mansoori (1975) points out the fact that the range of variation of Pd_o for cell protoplasm is 0 to 10^{-2}. Consequently, he concludes on the basis of analyzing the effects of intracellular nonuniform temperature distributions upon the kinetics of cell water loss during freezing, that the heat transfer process within the intracellular solution is only important for those cells which have a relatively low water content prior to the start of the cooling process. For yeast, with an initial total cell water content of 80.4%, temperature uniformity should be maintained intracellularly during freezing on the stage of a cryomicroscope.

2. *Extracellular Thermodynamic Equilibrium*

Since the yeast cell suspensions being frozen were dilute suspensions of yeast in distilled water, the assumption of a latent heat of fusion for the extracellular solution equal to that of pure water in deriving Eq. (16) is quite reasonable. Furthermore, the continual maintenance of thermodynamic equilibrium between the water and ice extracellularly as the temperature is changed is supported by the work of Stephenson (1960) and is discussed in great detail by Mazur (1963*b*).

Finally, it was assumed that, since the extracellular solution for the yeast cells was originally distilled water, no extracellular eutectic mixture was formed during cooling in the temperature range of between 0 and −30 °C. However, even if an extracellular eutectic mixture formed at temperatures, for example, below the KCl eutectic temperature of −10 °C, the extracellular solution osmolality would still be in excess of 5,000 mosmol/liter and thereby result in an equilibrium relative cell volume of only 32%. Consequently, formation of an extracellular eutec-

tic mixture cannot be used to explain the relatively larger cell volumes observed by Ushiyama and Cravalho at low temperatures for the lower cooling rates.

3. *Ideal, Dilute Intracellular Solution*

In the analysis it was assumed that the intracellular solution was both ideal and dilute. In reality, however, intracellular solutions are in general far from being either ideal or dilute. Nevertheless, Levin *et al.* (1976*b*, 1977*c*) have shown that solution nonideality and nondiluteness effects to a large extent can be lumped into the nonosmotic volume term $\hat{V}_b$ discussed previously, with the result being that equilibrium cell volumes as a function of solution osmolality obey the modified form of the Boyle-Van't Hoff relationship derived above [*see* Eq. (28) and Dick, 1959]. Furthermore, in cases where solution nonideality and nondiluteness have been included in the analysis of the kinetics of cell water loss during freezing, the effect that these phenomena have on cell volume at subzero temperatures have proved to be negligible (Mansoori, 1975; Levin *et al.*, 1977*c*). Specifically, yeast cells have been shown to obey the Boyle-Van't Hoff relationship (*see* previous discussion); and frozen suspensions of yeast have been found to absorb heat during warming in a similar manner to that shown for solutions which are known to be essentially both ideal and dilute (Mazur, 1963*a*).

4. *Uniform Spatial Distribution of Solutes; Absence of Unstirred Layers*

In the preceding analysis we have assumed that the spatial distributions of solutes remain uniform throughout both the intracellular and extracellular solutions during the cooling process. As Levin *et al.* (1977*a*) indicate, the governing nondimensional parmeter affecting the concentration polarization of solutes within solutions, i.e., formation of unstirred layers, is the Peclet number, Pec:

$$\text{Pec} = \frac{(\bar{v}_w J_w)\, l}{D^v} \tag{B2}$$

where $(\bar{v}_w J_w)$ is the water volume flux, l is the characteristic length of the system and D^v is the volume diffusivity of the solutes within the solution. If $\mathrm{Pec} \gg 1$, then the water transport process will be rate-limited by the mutual diffusion of solutes and solvent resulting in a nonuniform distribution of solutes within the solution. On the other hand, if $\mathrm{Pec} \ll 1$, then the water transport process will be rate-limited by the movement of water through the membrane and no nonuniform solute concentration profiles will be formed. The maximum water volume flux for the yeast cells that we are considering occurs at approximately $-10\,^{\circ}\mathrm{C}$ for the $100\,^{\circ}\mathrm{C}/\mathrm{min}$ cooling rate case and is of the order of $7.5 \times 10^{-6}\,\mathrm{cm/sec}$. Consequently, if the volume diffusivity of the intracellular solutes can be approximated by the diffusion coefficient of globular proteins in an aqueous solution, $D^v_{-30\,^{\circ}\mathrm{C}} \sim 8 \times 10^{-8}\,\mathrm{cm^2/sec}$ (Levin *et al.*, 1977*b*), and the characteristic length by $l \sim V_c/A_c \sim 1\,\mu\mathrm{m}$, then the Peclet number for the intracellular solution will be approximately 10^{-2}. If the volume diffusivity of whatever extracellular solutes which might exist can be approximated by the diffusion coefficient of simple salts in aqueous solutions, $D^v_{-30\,^{\circ}\mathrm{C}} \sim 1 \times 10^{-6}\,\mathrm{cm^2/sec}$, and the characteristic length by $l \sim 50\,\mu\mathrm{m}$, which is equivalent to a sphere with a diameter ten times that of an average yeast cell, then the Peclet number for the extracellular solution will be approximately 2×10^{-2}. Hence, essentially no concentration polarization of solutes should occur in either the intracellular or extracellular solutions.

5. *Compartmentalization*

So far in our discussion of the kinetics of cell water loss from yeast during freezing, we have only considered the lumped parameter case where both the cytoplasm and intra-vacuole solution lose an *equivalent* amount of water, resulting in the overall spatially uniform decrease in cell volume during cooling. That is, we have only considered the case where the tonoplast exerts a negligible influence upon the water transport process. However, if the tonoplast was the rate-limiting barrier in the overall permeation process then it would be possible, to cite an extreme example, for the cytoplasm to lose almost all of its free water while almost no water had left the vacuole. The overall cell volume in this instance would still decrease, but not uniformly. To test this compartmentalization hypothesis the following thermodynamic model was

employed with the MNLRA technique outlined above:

$$\frac{dV_c}{dt} = L_p^{MW} A_c RT(\Delta p - \Delta C^{MW})$$

and (B3)

$$\frac{dV_v}{dt} = -L_p^T A_v RT \Delta C^T$$

where V_c and A_c are the cell volume and surface area, V_v and A_v are the vacuole volume and tonoplast surface area, L_p^{MW} is the overall water permeability of the plasmalemma and cell wall, L_p^T is the water permeability of the tonoplast, ΔC^{MW} is the difference in osmolality between the extracellular solution and the cytoplasm, and ΔC^T is the difference in osmolality between the cytoplasm and the intra-vacuole solution. This model assumes that the tonoplast is semi-permeable and is incapable of supporting a hydrostatic pressure difference between the vacuole and the cytoplasm. Using Mazur's (1961*c*) values of 14% and 26% for the concentration of solids within the vacuole and cytoplasm, respectively, values for the osmotically inactive volume V_b and number of solute molecules N_s can be derived for both the intra-vacuole solution and the cytoplasm (Mazur, 1961*c*). Implementation of this model, however, led to extremely large values for the tonoplast water permeability, as opposed to almost the same values for the plasmalemma-cell wall permeability as were found for the simpler limped parameter case. Consequently, on the basis of these results we conclude that the yeast cell *S. cerevisiae* should shrink uniformly during the cooling process and that the yeast cell tonoplast exerts a negligible influence upon the overall water permeability process.

6. *Intact, Semi-Permeable Cell Membrane*

In the analysis, the plasmalemma and cell wall were assumed to remain intact and retain their overall semi-permeable properties during cooling. These assumptions are supported by electrical conductivity measurements (Mazur, 1963*a*) and interferometric measurements (Mazur, 1961*c*) on the same strain of *S. cerevisiae* used by Ushiyama and Cravalho. Moreover, the electrical resistivity measurements made by Mazur (1963*a*) suggest that the plasmalemma remains relatively impermeable to solutes during the cooling procedure and most of the

subsequent warming procedure even when the yeast are killed by their exposure to low temperatures. Finally, it should be noted that even at room temperature, the "leakage" rate of potassium in yeast is only 1% per hr (Rothstein, 1959) which is much too low to affect any of the results presented here. Consequently, on the basis of existing experimental data on *S. cerevisiae*, leakage of solutes, if present extracellularly, into the cell during freezing should not be significant and probably is not responsible for the relatively larger cell volumes experimentally seen by Ushiyama and Cravalho at the lower cooling rates.

7. *State of the Intracellular Solution*

On the basis of the above conclusions regarding the retention of the semipermeable characteristics of the yeast cell plasma membrane during cooling, the number of moles of solute N_s^I within the cell should remain constant as long as there is sufficient intracellular water to keep the solutes in solution. Mazur's electrical resistivity measurements of frozen yeast suspensions (1963*a*) indicate that liquid solution is present intracellularly even at $-30\,°C$ and his differential thermal analysis studies (Mazur, 1963*a*) indicate that most, if not all, of the intracellular solute molecules are in solution at temperatures above $-10\,°C$. Consequently, we feel that we are justified in making this assumption since only an increase in the number of intracellular solute molecules could result in more water being retained by the cell at the low temperatures. A decrease in N_s^I by the precipitation of solutes would have essentially no effect upon the value for V_b and only a slight effect upon the driving force for the water flux since at $-10\,°C$ the extracellular osmolality already exceeds the intracellular osmolality by an order of magnitude.

8. *Variation of* ε, V_b *and* A_c

Various arguments have already been presented to justify our use of the biophysical parameters presented in Table 2. It is therefore sufficient for us to say at this point that a value of 4.7 MPa (680 psi) or 2.2 MPa (220 psi) rather than zero for the volumetric elastic modulus, ε, had negligible effect ($\lesssim 10\%$) upon the permeability parameters found by using the thermodynamic model and the MNLRA technique outlined above. For example, by assuming that $\varepsilon = 4.7$ MPa instead of zero for the

10 °C/min cooling rate case, $L_{p)T_g}$ and E_{L_p} were found to be 1.1 $\times 10^{-13}$ cm/dynes and 63 kJ/mol, respectively, rather than 1.2 $\times 10^{-13}$ cm^3/dynes and 68 kJ/mol. An assumption of a constant cell surface area rather than a 2/3rds power dependence of A_c upon V_c and a value for the osmotically inactive volume, V_b, of 0.30 rather than 0.24, also had negligible ($\lesssim 10\%$) effect upon the resulting permeability parameters.

9. Nonsimple Osmolality and Temperature Dependence for L_p

As we have already mentioned, there is no *a priori* reason to believe that the temperature dependence of L_p is completely represented by the simple Arrhenius expression presented above [Eq. (17)]. Consequently, various combinations of series and parallel membrane resistances, each with different pre-exponential and exponential (apparent activation energy) terms, were used with the thermodynamic model and MNLRA technique outlined above. In all cases, the regression analysis indicated that the water transport process was rate-limited by only *a single* permeability barrier although on the basis of the available data it could not specifically identify that barrier.

References

Bank, H. 1973. Visualization of freezing damage. II. Structural alterations during warming. *Cryobiology* **10**:157

Bank, H. 1974. Freezing injury in tissue cultured cells as visualized by freeze etching. *Exp. Cell Res.* **85**:367

Bank, H., Mazur, P. 1973. Visualization of freezing damage. *J. Cell Biol.* **57**:729

Bevington, P.R. 1969. Data Reduction and Error Analysis for the Physical Sciences. McGraw-Hill, New York

Conway, E.J., Armstrong, W. McD. 1961. The total intracellular concentration of solutes in yeast and other plant cells and the distensibility of the plant-cell wall. *Biochem. J.* **81**:631

Conway, E.J., Downey, M. 1950. An outer metabolic region of the yeast cell. *Biochem. J.* **47**:347

Dainty, J. 1976. Water relations of plant cells. *In:* Transport in Plants II, Part A, Cells. U. Luttge and M.G. Pitman, editors. Springer-Verlag, Berlin

Dainty, J., Ginsburg, B.Z. 1964. The measurement of hydraulic conductivity (osmotic permeability to water) of internodal Characean cells by means of transcellular osmosis. *Biochim. Biophys. Acta* **79**:112

Dengel, O., Riehl, N. 1963. Diffusion von Protenen (Tritonen) in Eiskristallen. *Phys. Kondens. Mater.* **1**:191

Dick, D.A.T. 1959. Cell Water. Butterworth, London
Diller, K.R. 1975. Intracellular freezing: Effect of extracellular supercooling. *Cryobiology* **12**:480
Diller, K.R., Cravalho, E.G. 1970. A cryo-microscope for the study of freezing and thawing processes in biological cells. *Cryobiology* **7**:191
Diller, K.R., Cravalho, E.G., Huggins, C.E. 1976. An experimental study of intracellular freezing in erythrocytes. *Med. Biol. Eng.* **14**:321
Dorsey, N.E. 1940. Properties of Ordinary Water Substance. Reinhold, New York
Eddy, A.A., Williamson, D.H. 1957. A method of isolating protoplasts from yeast. *Nature (London)* **179**:1252
Farrant, J., Woolgar, A.E. 1972*a*. Human red cells under hypertonic conditions; A model system for investigating freezing damage. 1. Sodium chloride. *Cryobiology* **9**:9
Farrant, J., Woolgar, A.E. 1972*b*. Human red cells under hypertonic conditions; a model system for investigating freezing damage. 2. Sucrose. *Cryobiology* **9**:16
Hempling, H.G. 1960. Permeability of the Ehrlich ascites tumor cells to water. *J. Gen. Physiol.* **44**:365
House, C.R. 1974. Water Transport in Cells and Tissue. Williams & Wilkins, Baltimore
Itagaki, K. 1964. Self-diffusion in single-crystals of ice. *J. Phys. Soc. Jpn.* **19**:1081
Kelly, R.B., Kohn, P.G., Dainty, J. 1963. Water relations of *Nitella Translucens*. *Bot. Soc. Edinburgh Trans.* **39 (IV)**:373
Knox, J.M., Diller, K.R. 1977. Computer analysis of volumetric changes during cellular freezing-thawing. *Cryobiology* **14**:682
Leibo, S.P. 1977. Fundamental cryobiology of mouse ova and embryos. The freezing of mammalian embryos. *Ciba Found. Symp.* **52**:69
Leibo, S.P., McGrath, J.J., Cravalho, E.G. 1978. Microscopic observation of intracellular ice formation in unfertilized mouse ova as a function of cooling rate. *Cryobiology* **15**:257
Leibo, S.P., Rall, W.F., Mazur, P. 1977. Comparison of the observed and calculated water loss from mouse ova at subzero temperatures. *Cryobiology* **14**:703
Levin, R.L., Cravalho, E.G., Huggins,, C.E. 1976*a*. A membrane model describing the effect of temperature on the water conductivity of erythrocyte membranes at subzero temperatures. *Cryobiology* **13**:415
Levin, R.L., Cravalho, E.G., Huggins, C.E. 1976*b*. The effect of hydration on the water content of human erythrocytes. *Biophys. J.* **16**:1411
Levin, R.L., Cravalho, E.G., Huggins, C.E. 1977*a*. Diffusion in a liquid solution with a moving semi-permeable boundary. *J. Heat Transfer* **99**:322
Levin, R.L., Cravalho, E.G., Huggins, C.E. 1977*b*. The concentration polarization effect in frozen erythrocytes. *J. Biomech. Eng.* **99**:65
Levin, R.L., Cravalho, E.G., Huggins, C.E., 1977*c*. The effect of solution nonideality on RBC volume regulation. *Biochim. Biophys. Acta* **465**:179
Levin, R.L., Cravalho, E.G., Huggins, C.E. 1977*d*. Water transport in a cluster of closely-packed erythrocytes at subzero temperatures. *Cryobiology* **14**:549
Levin, S.W., Levin, R.L., Solomon, A.K. 1978. Permeability of human red cells and ghosts to water. *J. Gen. Physiol. (in press)*
Levin, R.L., Solomon, A.K. 1978. Permeability of human red cells to urea and water. *Biophys. J.* **21**:10*a*
Luikov, A.V. 1968. Analytical Heat Diffusion. Academic Press, New York
Mansoori, G.A. 1975. Kinetics of water loss from cells at subzero centigrade temperatures. *Cryobiology* **12**:34
Marquardt, D.W. 1963. An algorithm for least-squares estimation of nonlinear parameters. *J. Soc. Ind. Appl. Math.* **11**:431

Mazur, P. 1960. Physical factors implicated in the death of microorganisms at subzero temperatures. *Ann. N.Y. Acad. Sci.* **85**:610

Mazur, P. 1961*a*. Physical and temporal factors involved in the death of yeast at subzero temperatures. *Biophy. J.* **1**:247

Mazur, P. 1961*b*. Manifestations of injury in yeast cells exposed to subzero temperatures. I. Morphological changes in freeze-substituted and in "frozen-thawed" cells. *J. Bacteriol.* **82**:662

Mazur, P. 1961*c*. Manifestations of injury in yeast cells exposed to subzero temperatures. II. Changes in specific gravity and in the concentration and quantity of cell solids. *J. Bacteriol.* **82**:673

Mazur, P. 1963*a*. Studies on rapidly frozen suspensions of yeast cells by differential thermal analysis and conductometry. *Biophys. J.* **3**:343

Mazur, P. 1963*b*. Kinetics of water loss from cells at subzero temperatures and the likelihood of intracellular freezing. *J. Gen. Physiol.* **47**:347

Mazur, P. 1965. The role of cell membranes in the freezing of yeast and other single cells. *Ann. N.Y. Acad. Sci.* **125**:658

Mazur, P. 1977. The role of intracellular freezing in the death of cells cooled at supraoptimal rates. *Cryobiology* **14**:251

Mazur, P., Leibo, S.P., Chu, E.H.Y. 1972. A two-factor hypothesis of freezing injury – evidence from Chinese hamster tissue culture cells. *Exp. Cell Res.* **71**:345

McCutchen, M., Lucké, B. 1932. The effect of temperature on the permeability to water of resting and of activated cells (unfertilized and fertilized eggs of *Arbacia punctulata*). *J. Cell. Comp. Physiol.* **2**:11

McGrath, J.J., Cravalho, E.G., Huggins, C.E. 1975. An experimental comparison of intracellular ice formation and freeze-thaw survival of HeLa *S*-3 cells. *Cryobiology* **12**:540

Melchior, D.L., Steim, J.M. 1978. Lipid associated thermal effects in biomembranes. Progress in Surface and Membrane Science. Vol. 13. D.A. Cadenhead and J.F. Danielli, editors. Academic Press, New York

Meryman, H.T., Williams, R.J., Douglas, M.St.J. 1977. Freezing injury from "solution effects" and its prevention by natural or artificial cryoprotection. *Cryobiology* **14**:287

Ørskow, S.L. 1945. Investigations on the permeability of yeast cells. *Acta Pathol. Microbiol. Scand.* **22**:523

Papanek, T.H. 1978. The water permeability of the human erythrocyte in the temperature range +25 °C to −10 °C. Ph.D. Thesis. Massachusetts Institute of Technology, Cambridge

Philip, J.R. 1958. The osmotic cell, solute diffusibility and the plant water economy. *Plant Physiol.* **33**:264

Pushkar, N.S., Etkin, Y.A., Brønstein, V.L., Gordiyenko, E.A., Kozmin, Y.V., 1976. On the problem of dehydration and intracellular crystallization during freezing of cell suspensions. *Cryobiology* **13**:147

Rich, G.T., Sha'afi, R.I., Ronaldez, A., Solomon, A.K. 1968. Effect of osmolarity on the hydraulic permeability coefficient of red cells. *J. Gen. Physiol.* **52**:941

Robinson, R.A., Stokes, R.H. 1959. Electrolyte Solutions. (2nd ed.) Butterworth, London

Rothstein, A. 1959. Role of the cell membrane in the metabolism of inorganic electrolytes by microorganisms. *Bacteriol. Rev.* **23**:175

Sidel, V.W., Solomon, A.K. 1957. Entrance of water into human red cells under an osmotic pressure gradient. *J. Gen. Physiol.* **41**:243

Silvares, O.M., Cravalho, E.G., Toscano, W.M., Huggins, C.E. 1975. The thermodynamics of water transport for biological cells during freezing. *J. Heat Transfer* **97**:582

Stephenson, J.L. 1960. Ice crystal formation in biological materials during rapid freezing. *Ann. N. Y. Acad. Sci.* **85**:535

Steudle, E., Zimmermann, U., Luttge, U. 1977. Effect of turgor pressure and cell size on the wall elasticity of plant cells. *Plant Physiol.* **59**:285

Stusnick, E., Hurst, R.P. 1972. Numerical determination of membrane permeability parameters. *J. Theor. Biol.* **37**:261

Ushiyama, M. 1973. Volumetric changes in *Saccharomyces cerevisiae* during freezing at constant cooling velocities. S.M. Thesis. Massachusetts Institute of Technology, Cambridge

Ushiyama, M., Cravalho, E.G., Diller, K.R., Huggins, C.E. 1973. Intracellular water content of *Saccharomyces cerevisiae* during freezing at constant cooling rates. *Cryobiology* **10**:517

Watson, W.W. 1974. Volumetric changes in human erythrocytes during freezing at constant cooling velocities. S.M. Thesis. Massachusetts Institute of Technology, Cambridge

Watson, W.W., Diller, K.R., Cravalho, E.G., Huggins, C.E. 1974. Volumetric changes in human erythrocytes during freezing at constant cooling rates. *Cryobiology* **11**:519

Wiest, S.C., Steponkus, P.L., 1978. Freeze-thaw injury to isolated spinach protoplasts and its simulation at above freezing temperatures. *Plant Physiol.* **62**:699

Wood, T.H., Rosenberg, A.M. 1957. Freezing in yeast cells. *Biochim. Biophys. Acta* **25**:78